

An exponential random graph modeling approach to creating group-based representative whole-brain connectivity networks

Sean L. Simpson^{a,*}, Malaak N. Moussa^b, Paul J. Laurienti^c

^a Department of Biostatistical Sciences, Wake Forest University School of Medicine Winston-Salem, NC, USA

^b Neuroscience Program, Wake Forest University School of Medicine Winston-Salem, NC, USA

^c Department of Radiology, Wake Forest University School of Medicine Winston-Salem, NC, USA

*Corresponding author. Department of Biostatistical Sciences, Wake Forest University School of Medicine, Medical Center Boulevard, Winston-Salem, NC 27157, USA. Fax: +1 336 716 6427.

E-mail address: slsimpso@wfubmc.edu (S. Simpson).

ABSTRACT

Group-based brain connectivity networks have great appeal for researchers interested in gaining further insight into complex brain function and how it changes across different mental states and disease conditions. Accurately constructing these networks presents a daunting challenge given the difficulties associated with accounting for inter-subject topological variability. Viable approaches to this task must engender networks that capture the constitutive topological properties of the group of subjects' networks that it is aiming to represent. The conventional approach has been to use a *mean* or *median* correlation network (Achard et al., 2006; Song et al., 2009) to embody a group of networks. However, the degree to which their topological properties conform with those of the groups that they are purported to represent has yet to be explored. Here we investigate the performance of these *mean* and *median* correlation networks. We also propose an alternative approach based on an exponential random graph modeling framework and compare its performance to that of the aforementioned conventional approach. Simpson et al. (2010) illustrated the utility of exponential random graph models (ERGMs) for creating brain networks that capture the topological characteristics of a single subject's brain network. However, their advantageousness in the context of producing a brain network that "represents" a group of brain networks has yet to be examined. Here we show that our proposed ERGM approach outperforms the conventional *mean* and *median* correlation based approaches and provides an accurate and flexible method for constructing group-based representative brain networks.

Keywords: ERGM; p-star; Brain; Network; Small-world; fMRI.

Introduction

Whole-brain connectivity analysis is a burgeoning area in neuroscience which is gaining prominence due to the need to understand how various regions of the brain interact with one another. The application of network and graph theory has facilitated these analyses and enabled examining the brain as an integrated system rather than a collection of individual components (Bullmore and Sporns, 2009). Despite the utility of network science in providing insight into the infrastructural properties of a given subject's brain, capturing and understanding these properties in a group of subjects has been challenging and has slowed research focusing on changes in complex brain function across different cognitive and disease states.

As noted in Rubinov and Sporns (2010), comparing brain networks across subjects and groups of subjects necessitates the development of accurate statistical comparison tools. Despite this need, the amount of work done in this area has not been commensurate with its level of importance (van Wijk et al., 2010). Network-based statistics (NBS), like that of Zalesky et al. (2010), have been proposed for identifying edge-based or component-based differences in brain networks. However, these approaches have been inherently univariate, leaving the complex dependence structure of the networks largely unaccounted for. They also fail to provide a way to create group based networks that represent the topological characteristics of the subjects' networks. Developing an analytical approach to capture the network characteristics from a group of subjects' brain networks has great appeal and would help to fill the gap in the group comparison literature. These group-based brain connectivity networks could serve as null networks against which other networks and network models can be compared, as visualization tools, and as a means for characterizing properties of network metrics in a group (e.g., community structure) (Joyce et al., 2010; Meunier et al., 2009a,b; Valencia et al., 2009). However, creating these group-based "representative" networks is a daunting challenge given the difficulties associated with accounting for the inter-subject topological variability.

Thus far, researchers have taken one of three general approaches to generating a group-based representative functional network. The most common method has been to take the mean of the functional connectivity matrices of the subjects in a group and threshold this group mean matrix to get a *mean* network (Achard et al., 2006; Meunier et al., 2009a,b; Valencia et al., 2009). Although this approach is intuitive and computationally straight forward, as with use of the mean in any context, the resulting network may be unduly influenced by one or more outlying functional connectivity values. Additionally, this approach is *edge-based* since the averaging is done across the individual entries of the connectivity matrices; and thus, it ignores the topological properties of each subject's network. Another similar approach taken by researchers is to take the median of the functional connectivity matrices of the subjects and threshold this group median matrix to get a *median* network (Song et al., 2009). While this approach provides more robustness to outlying connectivity values, it is still *edge-based* and ignores the topological dependence among edges within each subject's network. A third, and more contrasting approach, was taken by Meunier et al. (2009) and Joyce et al. (2010). They used a *best subject* network to represent the group by assessing between subject differences in network organization and identifying the most representative subject in the sample. However, it would be ideal to have a method that incorporates the data from all subjects directly, like the *mean* and *median edge-based* network approaches, while also capturing the constitutive topological properties of these subjects' networks. Toward this end, we propose an approach to creating group-based representative networks that utilizes exponential random graph models (ERGMs), also known as p^* models (Frank and Strauss, 1986; Wasserman and Pattison, 1996; Robins et al., 1999; Pattison and Wasserman, 1999). These models enable achieving an efficient representation of complex network data structures by modeling a network's global structure as a function of local topological features.

Simpson et al. (2010) showed the utility of ERGMs for simulating a brain network that retains the constitutive properties of a single subject's original network. However, their usefulness in producing a brain network that "represents" the topological characteristics of a group of networks has yet to be explored. Also, despite the frequent use of *mean* and *median* group-based networks, the amount to which their topological properties coincide with those of the groups that they are purported to represent has yet to be investigated. Here we make use of resting-state

fMRI data from ten normal subjects to 1) examine how well the mean and median approaches capture important topological properties of the group and 2) compare their performances to our ERGM approach.

Materials and methods

Data and network construction

Our analysis included fMRI data from 10 normal subjects (5 female, average age 27.7 years old [4.7 SD]). For each subject, 120 images were acquired during 5 minutes of resting using a gradient echo echoplanar imaging (EPI) protocol with TR/TE=2500/40 ms on a 1.5 T GE twin-speed LX scanner with a birdcage head coil (GE Medical Systems, Milwaukee, WI). The acquired images were motion corrected, spatially normalized to the MNI (Montreal Neurological Institute) space and re-sliced to 4×4×5 mm voxel size using an in-house processing script based on SPM99 package (Wellcome Trust Centre for Neuroimaging, London, UK). The resulting images were not smoothed in order to avoid artificially introducing local spatial correlation (van den Heuvel et al., 2008). These subjects were part of a larger study with further details provided in Peiffer et al. (2009).

The first step in performing the network construction was to calculate Pearson partial correlation coefficients between the time courses of all node pairs adjusted for motion and physiological noises (see Hayasaka and Laurienti, 2010 for further details). These node time courses were obtained by averaging the voxel time courses in the 90 distinct anatomical regions (90 ROIs-Regions of Interest) defined by the Automated Anatomical Labeling atlas (AAL; Tzourio-Mazoyer et al., 2002). Three types of networks were then generated based on the resulting 90×90 correlation matrices. Unweighted, undirected *subject-specific* networks (an example of which is shown in Figure 1) were created by thresholding the correlation matrices for each subject to yield a set of adjacency matrices (\mathbf{A}_{ij}) with 1 indicating the presence and 0 indicating the absence of an edge between two nodes. A group-based *mean* network was constructed by averaging the correlation matrices of the 10 subjects (i.e., averaging element (i,j) across matrices) and then thresholding the resulting matrix to yield a mean adjacency matrix. Similarly, a group-based *median* network was produced by computing the median of element (i,j) across the 10 correlation matrices and then thresholding the resulting matrix. All networks were defined (thresholded) so that the relationship between the number of nodes n and the average node degree K is the same across networks. In particular, the networks were defined so that $S = \log(n)/\log(K) = 2.8$ (see Hayasaka and Laurienti, 2010 for further details on this thresholding approach).

Model definition

Exponential random graph models (ERGMs) have the following form (Handcock, 2002):

$$P_{\theta}(\mathbf{Y} = \mathbf{y}) = \kappa(\theta)^{-1} \exp\{\theta^T \mathbf{g}(\mathbf{y})\} \quad (1)$$

Here \mathbf{Y} is an $n \times n$ (n nodes) random symmetric adjacency matrix representing a brain network from a particular class of networks, with $\mathbf{Y}_{ij} = 1$ if an edge exists between nodes i and j and $\mathbf{Y}_{ij} = 0$ otherwise. We statistically model the probability mass function (pmf) ($P_{\theta}(\mathbf{Y} = \mathbf{y})$) of this class

of networks as a function of the prespecified network features defined by the p -dimensional vector $\mathbf{g}(\mathbf{y})$. This vector of explanatory metrics can contain any graph statistic (e.g., number of edges) or node statistic (e.g., brain location of the node). The goal in defining $\mathbf{g}(\mathbf{y})$ is to identify local metrics that concisely summarize the global (whole-brain) structure. A subset of mathematically compatible metrics for ERGMs is defined in Table 1 (Morris et al., 2008). The parameter vector $\boldsymbol{\theta} \in \mathbb{R}^p$ (which must be estimated), associated with $\mathbf{g}(\mathbf{y})$, quantifies the relative significance of each network feature in explaining the structure of the network after accounting for the contribution of all other network features in the model. The normalizing constant $\kappa(\boldsymbol{\theta})$ ensures that the probabilities sum to one. This approach allows representing the global network structure (\mathbf{y}) by locally specified explanatory metrics ($\mathbf{g}(\mathbf{y})$), and is capable of capturing several important topological properties of brain networks simultaneously (Simpson et al., 2010). The fitted parameter values ($\boldsymbol{\theta}$) can then be utilized to understand particular emergent behaviors of the network (how local features give rise to the global structure).

Estimation of the model parameters $\boldsymbol{\theta}$ is normally done with either Markov chain Monte Carlo maximum likelihood estimation (MCMC MLE) or maximum pseudo-likelihood estimation (MPLE) (van Duijn et al., 2009 contains details). Model fits with MPLE are much simpler computationally than MCMC MLE fits and afford higher convergence rates with large networks. However, properties of the MPLE estimators are not well understood, and the estimates tend to be less accurate than those of MCMC MLE. Here we employ MCMC MLE to fit the model in equation 1 given that there were no convergence issues. Hunter et al. (2008b) provides further details about this estimation approach which can be implemented in the *statnet* package (Handcock et al., 2008) for the R statistical computing environment.

Representative network creation

In order to create a group-based representative network via ERGMs, it is necessary to get a group-based summary measure of the fitted parameter values ($\boldsymbol{\theta}$) for all subjects. The first step in this process involves identifying the most important explanatory metrics ($\mathbf{g}(\mathbf{y})$) for each subject's network as done in Simpson et al. (2010). They implemented a graphical goodness of fit (GOF) approach (Hunter et al., 2008a) to select the “best” metrics from the set of potential metrics listed by category in Table 2. These categories were chosen based on properties of brain networks that are regarded as important in the literature (Bullmore and Sporns, 2009). Further details on the metrics are provided in Table 1 and Morris et al. (2008). The bolded metrics (Edges, GWESP, and GWNSP) in Table 2 were those contained in at least half (≥ 5) of the resulting sets of best explanatory metrics for the subjects. Examining the uniformity of the selected explanatory metrics across subjects in this way is important due to metric interdependencies. In other words, for example, the fitted parameter value (θ_{edge}) associated with the Edge metric in a given subject's model is statistically dependent upon/accounts for all other fitted parameter values in the model. Thus, an appropriate statistical comparison or summary of θ_{edge} across subjects requires that the fitted ERGMs for all subjects contain the same set of metrics ($\mathbf{g}(\mathbf{y})$).

Given the bolded metrics in Table 2, the second step in creating our group-based representative networks was to refit the networks of all 10 subjects with the “best” group model

$$P_{\boldsymbol{\theta}}(\mathbf{Y} = \mathbf{y}) = \kappa(\boldsymbol{\theta})^{-1} \exp\{\theta_1 \text{Edges} + \theta_2 \text{GWESP} + \theta_3 \text{GWNSP}\}. \quad (2)$$

The estimated parameter values $(\theta_1, \theta_2, \theta_3)$ are displayed in Table 3 along with the mean and median of those values across subjects. We then employed these mean $(\bar{\theta}_1, \bar{\theta}_2, \bar{\theta}_3)$ and median $(\tilde{\theta}_1, \tilde{\theta}_2, \tilde{\theta}_3)$ values to simulate random realizations of networks from their corresponding probability mass functions below:

$$P_{\theta}(\mathbf{Y} = \mathbf{y}) = \kappa(\boldsymbol{\theta})^{-1} \exp\{\bar{\theta}_1 \text{Edges} + \bar{\theta}_2 \text{GWESP} + \bar{\theta}_3 \text{GWNSP}\} \quad (3)$$

$$P_{\theta}(\mathbf{Y} = \mathbf{y}) = \kappa(\boldsymbol{\theta})^{-1} \exp\{\tilde{\theta}_1 \text{Edges} + \tilde{\theta}_2 \text{GWESP} + \tilde{\theta}_3 \text{GWNSP}\}. \quad (4)$$

Five *mean ERGM* and five *median ERGM* based networks were simulated based on equations 3 and 4 respectively. Additionally, five more networks were simulated from each probability mass function (in equations 3 and 4) where the degree distributions were constrained to have the same distribution as subject 16 whom we deemed to be most representative of the group in terms of this metric. Accurately capturing the degree distribution of a set of networks proved difficult; thus, given its importance in conferring vital properties to brain networks, this constrained simulation approach was taken to examine whether we could fix the degree distribution while still being able to properly represent other topological properties of the group. In total, then, we had 20 potential group-based representative networks generated from these simulations.

Network assessment

Neurobiologically relevant network metrics were calculated for all subjects' networks, the *mean* and *median* correlation networks, and all ERGM derived mean and median simulated networks. Unless otherwise noted, these metrics were calculated and evaluated using in-house processing scripts. A more detailed review of the metrics used in these analyses can be found in the literature (Rubinov and Sporns, 2010).

A commonly used measure of network connectivity, *degree* (K), was determined for each network. The *degree* for each node (k_i) in a network was computed as the total number of functional links that were associated with a node i . The *characteristic path length* (L) is a measure of the functional integration within a network and was calculated using Dijkstra's algorithm (Dijkstra, 1959) in the MatlabBGL package (David Gleich; Stanford University, Stanford, CA). It is equivalent to the average shortest path length in a network and was found by generating a matrix of the geodesic distances between all node pairs. However, in the case of isolated nodes and subgraphs this value is infinitely distant from the *largest network component* (N_c). Because of this, the harmonic mean of the geodesic distances was used to calculate L :

$$L = \frac{N(N-1)}{\sum_{i \neq j} \frac{1}{d_{ij}}} \quad (5)$$

where d_{ij} is equal to the harmonic mean of the geodesic distance between nodes i and j (Latora and Marchiori, 2001; Newman, 2002, 2003). *Global efficiency* (E_{glob}), which is the reciprocal of the *characteristic path length* (Latora and Marchiori, 2001), captures the level of distributive processing in a network. Unlike the *characteristic path length*, *global efficiency* is scaled and ranges in value from zero to one, where the latter represents maximal distributed processing.

Clustering coefficient (C) is defined as the fraction of triangles around a particular node in a network and is thus a measure of local network segregation (Watts and Strogatz, 1998). Akin to the *clustering coefficient* is *local efficiency* (E_{loc}). For each node in a network, this value represents the average local sub-graph efficiencies of its neighboring nodes (Latora and Marchiori, 2001). Like E_{glob} , it is a scaled value that ranges from zero to one. Nodes within a network with values closer to one are those with connections that are predominately local.

Assortativity (R_{jk}) captures the likelihood a node is connected with other like nodes in a network (Newman, 2002, 2003). In this study *assortativity* was based on similarity of node *degree*. Networks with values closer to 1 were defined as assortative and exhibited high-high and low-low degree connections. Values that were closer to -1 were indicative of disassortative networks with high-low degree connections.

The following analyses were done to compare original subject data to the *mean* and *median* correlation networks as well as the degree-constrained and non-constrained *mean ERGM* and *median ERGM* simulation-based networks. First, values from each of the 90-nodes of a subject's network were used to calculate whole-network means for each metric. The mean and median of these whole-network metric values for each subject were then computed across all subjects and compared with the corresponding metric values for the *mean* and *median* correlation networks and degree-constrained and non-constrained *mean ERGM* and *median ERGM* simulation-based networks. We also calculated the Euclidean distance between metric values of the networks in order to assess how well the representative networks captured all of the group mean and median topological values simultaneously. That is, we evaluated the square root of the squared distances between the group mean and median metric values and those of the *mean* and *median* correlation networks and degree-constrained and non-constrained *mean ERGM* and *median ERGM* simulation-based networks. Second, with the exception of *degree* and *assortativity*, the nodal cumulative distributions of each metric were generated for each network. These were made in order to evaluate which of the representative networks best captured the metric distributions of the subjects' data. Finally, to assess how well each representative network captured the nodal connectivity (*degree*) of the original subjects' networks, degree distributions were made. These log-log plots show the likelihood with which a particular node in a network displays a certain degree (Lima-Mendez and van Helden, 2009). Additionally, to visually assess whether or not representative networks could capture the overall topology of the original subjects' networks, Harel-Koren Fast Multiscale graphs (Harel and Koren, 2001) were plotted using NodeXL.

Results and Discussion

We implemented the network assessment procedure delineated in the previous section for the 20 *mean ERGM* and *median ERGM* simulation-based representative networks and compared the results to those of the frequently used *mean* and *median* networks based on the subjects' correlation matrices. Table 4 shows the results of this assessment and comparison for the 10 unconstrained and 10 constrained simulated networks. As evidenced by the results in Table 4a, the 10 unconstrained *mean ERGM* and *median ERGM* simulation-based representative networks more accurately capture the group mean and median values for path length (L), size of the giant component (N_c), mean degree (K), and global efficiency (E_{glob}) than the corresponding *mean* and *median* correlation networks. There are minimal differences in accuracy for clustering coefficient (C) and local efficiency (E_{loc}), with the *mean* and *median* correlation networks only being decisively more accurate for assortativity (R_{jk}). When assessing the accuracy in capturing all of

the group mean and median topological values simultaneously via the distance metric, all five of the unconstrained *mean ERGM* simulation-based networks outperform the *mean* correlation network, while four of the five *median ERGM* simulation-based networks outperform the *median* correlation network. However, since our ultimate goal is to select a network that is most representative of the group, only one simulation-based network need outperform the *mean* and *median* correlation networks for our approach to be useful. Thus, the anomalous underperforming *median ERGM* simulation-based network is of little relevance in our context. An examination of the degree distributions for the subjects' networks, unconstrained *mean ERGM* and *median ERGM* simulation-based networks, and *mean* and *median* correlation networks in Figure 2a illustrates the fact that the *mean* and *median* correlation networks tend to overestimate this distribution while the unconstrained *mean ERGM* and *median ERGM* simulation-based networks generally underestimate it.

Table 4b displays the results for the 10 constrained *mean ERGM* and *median ERGM* simulation-based networks. As was the case with the unconstrained networks, these constrained networks also more accurately capture the group mean and median values for path length (L) (though 4 of the 10 simulations do a fairly poor job), size of the giant component (N_c), mean degree (K) (by construction), and global efficiency (E_{glob}) than the corresponding *mean* and *median* correlation networks. Moreover, they are also more faithful to the group mean and median values for local efficiency (E_{loc}). There are minimal differences in accuracy for clustering coefficient (C), with the *mean* and *median* correlation networks again only being decisively more accurate for assortativity (R_{jk}); nevertheless, the *mean ERGM* and *median ERGM* simulation-based networks qualitatively capture the assortative behavior of the brain networks, but just overestimate it quantitatively. As evidenced by the distance metric, the 10 constrained *mean ERGM* and *median ERGM* simulation-based representative networks uniformly outperform the corresponding *mean* and *median* correlation networks. Figure 2b depicts the degree distributions of the constrained *mean ERGM* and *median ERGM* simulation-based networks along with those of the *mean* and *median* correlation networks and subjects' networks. By construction, the *mean ERGM* and *median ERGM* simulation-based networks have degree distributions that well represent (fall near the middle of) those of the group. Given this, and based on the results of Table 4, *mean ERGM* network #5 and *median ERGM* network #4 serve as the two best candidates for the group-based representative network.

In addition to capturing mean nodal properties as demonstrated in Table 4, it was also of interest to examine how well the best *mean ERGM* and *median ERGM* simulation-based representative networks (*mean ERGM* network #5 and *median ERGM* network #4) typified the distribution of these nodal properties. Figure 3 displays the nodal distributions of path length (L), clustering coefficient (C), global efficiency (E_{glob}), and local efficiency (E_{loc}) for the 10 subjects' networks, *mean* and *median* correlation networks, and *mean ERGM* network #5 and *median ERGM* network #4. The *mean ERGM* network #5 and *median ERGM* network #4 preserve the distribution of the nodal properties extremely well, clearly outperforming the *mean* and *median* correlation networks. The Harel-Koren Fast Multiscale graphs (Harel and Koren, 2001) in Figure 4 help to visualize the networks in two dimensions and provide further visual evidence that the *mean ERGM* network #5 and *median ERGM* network #4 better capture the constitutive properties of the subjects' networks than the *mean* and *median* correlation networks.

Conclusion

The construction of representative group-based networks is of paramount importance for brain network scientists. These networks can serve multiple purposes including (but not limited to) as null networks against which other networks and network models can be compared, as visualization tools, and as a means for characterizing properties of network metrics in a group (e.g., community structure). The work herein illustrates the utility of the ERGM framework for producing group-based representative networks that capture both important average topological properties and nodal distributions of those properties in a group of networks better than the commonly used *mean* and *median* correlation networks. Of the 20 networks simulated based on our approach, 19 outperformed the *mean* and *median* correlation networks as assessed by our distance metric, with the best two being an order of magnitude more accurate; though, again, only *one* network (the one with the smallest distance) would ultimately be chosen. The representative network produced within this framework has the potential to be further improved by simply increasing the number of simulations and thereby increasing the probability of producing a network with an even smaller distance value. Moreover, this approach can be further refined by developing and assessing additional explanatory metrics that may lead to a more descriptive group model (equation 2). It is important to note that our approach is ad hoc, and may not work in all cases. Also, the amount of programming work increases linearly with the number of subjects in the group since ERGMs must be fitted and assessed for each subject individually. However, in contexts where the method appears feasible, like the one presented here, our approach is clearly more appealing than the current methods.

Acknowledgements

This work was supported by the Translational Science Institute of Wake Forest University (Translational Scholar Award).

References

- Achard, S., Salvador, R., Whitcher, B., Suckling, J., Bullmore, E., 2006. A resilient, low-frequency, small-world human brain functional network with highly connected association cortical hubs. *Journal of Neuroscience* 26 (1), 63-72.
- Bullmore, E., Sporns, O., 2009. Complex brain networks: graph theoretical analysis of structural and functional systems. *Nat. Rev. Neurosci* 10 (3), 186-198.
- Dijkstra, E., 1959. A note on two problems in connexion with graphs. *Numer. Math.* 1, 269-271.
- Frank, O., Strauss, D., 1986. Markov Graphs. *Journal of the American Statistical Association* 81 (395), 832-842.
- Handcock, M.S., Hunter, D.R., Butts, C.T., Goodreau, S.M., Morris, M., 2008. statnet: Software Tools for the Representation, Visualization, Analysis and Simulation of Network Data. *J Stat Softw* 24 (1), 1548-7660.
- Harel, D., Koren, Y., 2001. A fast multi-scale method for drawing large graphs, in: *Graph drawing*. pp. 235–287.
- Hayasaka, S., Laurienti, P.J., 2010. Comparison of characteristics between region- and voxel-based network analyses in resting-state fMRI data. *Neuroimage* 50 (2), 499-508.
- Hunter, D.R., Handcock, M.S., Butts, C.T., Goodreau, S.M., Morris, M., 2008. ergm: A Package to Fit, Simulate and Diagnose Exponential-Family Models for Networks. *J Stat Softw* 24 (3), nihpa54860.

- Hunter, D., Goodreau, S., Handcock, M., 2008. Goodness of fit of social network models. *Journal of the American Statistical Association* 103 (481), 248-258.
- Joyce, K.E., Laurienti, P.J., Burdette, J.H., Hayasaka, S., 2010. A new measure of centrality for brain networks. *PLoS ONE* 5 (8), e12200.
- Latora, V., Marchiori, M., 2001. Efficient behavior of small-world networks. *Phys. Rev. Lett* 87 (19), 198701.
- Lima-Mendez, G., van Helden, J., 2009. The powerful law of the power law and other myths in network biology. *Mol Biosyst* 5 (12), 1482-1493.
- Meunier, D., Achard, S., Morcom, A., Bullmore, E., 2009a. Age-related changes in modular organization of human brain functional networks. *Neuroimage* 44 (3), 715-723.
- Meunier, D., Lambiotte, R., Fornito, A., Ersche, K.D., Bullmore, E.T., 2009b. Hierarchical modularity in human brain functional networks. *Front Neuroinformatics* 3, 37.
- Morris, M., Handcock, M.S., Hunter, D.R., 2008. Specification of Exponential-Family Random Graph Models: Terms and Computational Aspects. *J Stat Softw* 24 (4), 1548-7660.
- Newman, M.E.J., 2002. Assortative mixing in networks. *Phys. Rev. Lett* 89 (20), 208701.
- Newman, M.E.J., 2003. Mixing patterns in networks. *Phys Rev E Stat Nonlin Soft Matter Phys* 67 (2 Pt 2), 026126.
- Pattison, P., Wasserman, S., 1999. Logit models and logistic regressions for social networks: II. Multivariate relations. *British Journal of Mathematical & Statistical Psychology* 52, 169-193.
- Peiffer, A.M., Hugenschmidt, C.E., Maldjian, J.A., Casanova, R., Srikanth, R., Hayasaka, S., Burdette, J.H., Kraft, R.A., Laurienti, P.J., 2009. Aging and the interaction of sensory cortical function and structure. *Hum Brain Mapp* 30 (1), 228-240.
- Robins, G., Pattison, P., Wasserman, S., 1999. Logit models and logistic regressions for social networks: III. Valued relations. *Psychometrika* 64 (3), 371-394.
- Rubinov, M., Sporns, O., 2010. Complex network measures of brain connectivity: uses and interpretations. *Neuroimage* 52 (3), 1059-1069.
- Simpson, S.L., Hayasaka, S., Laurienti, P.J., 2010. Selecting an exponential random graph model for complex brain networks. 1007.3230.
- Song, M., Liu, Y., Zhou, Y., Wang, K., Yu, C., Jiang, T., 2009. Default network and intelligence difference. *Conf Proc IEEE Eng Med Biol Soc 2009*, 2212-2215.
- Tzourio-Mazoyer, N., Landeau, B., Papathanassiou, D., Crivello, F., Etard, O., Delcroix, N., Mazoyer, B., Joliot, M., 2002. Automated anatomical labeling of activations in SPM using a macroscopic anatomical parcellation of the MNI MRI single-subject brain. *Neuroimage* 15 (1), 273-289.
- Valencia, M., Pastor, M.A., Fernández-Seara, M.A., Artieda, J., Martinerie, J., Chavez, M., 2009. Complex modular structure of large-scale brain networks. *Chaos* 19 (2), 023119.
- Wasserman, S., Pattison, P., 1996. Logit models and logistic regressions for social networks .1. An introduction to Markov graphs and p^* . *Psychometrika* 61 (3), 401-425.
- Watts, D.J., Strogatz, S.H., 1998. Collective dynamics of 'small-world' networks. *Nature* 393 (6684), 440-442.
- van Duijn, M., Gile, K., Handcock, M., 2009. A framework for the comparison of maximum pseudo-likelihood and maximum likelihood estimation of exponential family random graph models. *Social Networks* 31 (1), 52-62.
- van den Heuvel, M.P., Stam, C.J., Boersma, M., Hulshoff Pol, H.E., 2008. Small-world and scale-free organization of voxel-based resting-state functional connectivity in the human

- brain. *Neuroimage* 43 (3), 528-539.
- van Wijk, B.C.M., Stam, C.J., Daffertshofer, A., 2010. Comparing brain networks of different size and connectivity density using graph theory. *PLoS ONE* 5 (10), e13701.
- Zalesky, A., Fornito, A., Bullmore, E.T., 2010. Network-based statistic: identifying differences in brain networks. *Neuroimage* 53 (4), 1197-1207.

Table 1
Subset of ERGM explanatory metrics

Metric	Description
Edges	Number of edges in the network
Two-Path	Number of paths of length 2 in the network
k-Cycle	Number of k-cycles in network
k-Degree	Number of nodes with degree k
Geometrically weighted degree (GWD)	Weighted sum of the counts of each degree (i) weighted by the geometric sequence $(1 - \exp\{-\tau\})^i$, where τ is a decay parameter
Geometrically weighted edge-wise shared partner (GWESP)	Weighted sum of the number of connected nodes having exactly i shared partners weighted by the geometric sequence $(1 - \exp\{-\tau\})^i$, where τ is a decay parameter
Geometrically weighted non-edge-wise shared partner (GWNSP)	Weighted sum of the number of non-connected nodes having exactly i shared partners weighted by the geometric sequence $(1 - \exp\{-\tau\})^i$, where τ is a decay parameter
Geometrically weighted dyad-wise shared partner (GWDSP)	Weighted sum of the number of dyads ^a having exactly i shared partners weighted by the geometric sequence $(1 - \exp\{-\tau\})^i$, where τ is a decay parameter
Nodematch	Number of edges (i,j) for which nodal attribute i equals nodal attribute j (e.g., brain location of node i = brain location of node j)

^anode pair with or without edge

Table 2

Explanatory network metrics by category

Category	Metric(s) ^b
1) Connectedness	Edges , Two-Path
2) Local Clustering/Efficiency	GWESP , GWDSP
3) Global Efficiency	GWNSP ^a
4) Degree Distribution	GWD
5) Location (in the brain)	Nodematch

^aNot inherently global, but helps produce models that accurately capture the global efficiency of our networks

^bBolded metrics were those contained in at least half of the "best" subject network models

Table 3

Group model parameter estimates

Subject	θ_1 (Edges)	θ_2 (GWESP)	θ_3 (GWNSP)
002	-2.562	0.966	-0.293
003	-1.842	0.745	-0.329
005	-2.789	1.016	-0.279
008	-3.367	1.311	-0.266
009	-3.287	1.092	-0.180
010	-3.666	1.335	-0.204
012	-2.549	0.973	-0.266
013	-2.791	1.044	-0.301
016	-2.525	0.951	-0.308
021	-2.316	0.704	-0.365
Mean	-2.769	1.014	-0.279
Median	-2.676	0.994	-0.286

Note: subject 2 results differ slightly from Simpson et al. (2010) due to a fix in the data processing.

Table 4

Network assessment results for the subjects' networks, edge-based *mean* and *median* correlation networks, and *mean ERGM* and *median ERGM* simulation-based networks.

a) Unconstrained *mean ERGM* and *median ERGM* simulation-based networks.

(A)		N_c	L	K	C	E_{loc}	E_{glob}	R_{jk}		
Subject										
	Mean	83.7	4.14	5.05	0.40	0.49	0.28	0.29		
	Median	84.5	4.18	5.04	0.41	0.49	0.28	0.30		
Edge-Based Network									Distance	
	Mean	89	3.54	6.42	0.44	0.55	0.35	0.33	5.51	
	Median	88	3.01	7.60	0.45	0.59	0.39	0.22	4.49	
ERGM Simulation										
	<i>Unconstrained</i>									
	Mean									
		<i>1</i>	85	4.48	4.09	0.37	0.45	0.26	0.11	1.66
		<i>2</i>	85	3.63	4.58	0.35	0.44	0.30	0.09	1.49
		<i>3</i>	83	4.12	3.76	0.39	0.45	0.26	0.12	1.48
		<i>4</i>	88	4.28	4.27	0.45	0.52	0.29	0.02	4.38
		<i>5</i>	83	4.59	3.84	0.40	0.47	0.24	0.20	1.47
	Median									
		<i>1</i>	86	3.93	4.62	0.34	0.41	0.30	0.40	1.58
		<i>2</i>	87	4.48	4.31	0.42	0.51	0.27	0.20	2.63
		<i>3</i>	86	4.35	4.64	0.42	0.49	0.28	0.39	1.57
		<i>4</i>	86	3.83	4.71	0.36	0.46	0.30	0.33	1.58
		<i>5</i>	78	4.72	3.78	0.43	0.49	0.22	0.20	6.65

b) Degree-constrained *mean ERGM* and *median ERGM* simulation-based networks.

(B)		N_c	L	K	C	E_{loc}	E_{glob}	R_{jk}		
Subject										
	Mean	83.7	4.14	5.05	0.40	0.49	0.28	0.29		
	Median	84.5	4.18	5.04	0.41	0.49	0.28	0.30		
Edge-Based Network									Distance	
	Mean	89	3.54	6.42	0.44	0.55	0.35	0.33	5.51	
	Median	88	3.01	7.60	0.45	0.59	0.39	0.22	4.49	
ERGM Simulation										
	<i>Constrained</i>									
	Mean									
		<i>1</i>	83	4.43	5.04	0.45	0.56	0.26	0.47	0.79
		<i>2</i>	83	5.51	5.04	0.43	0.51	0.23	0.61	1.57
		<i>3</i>	81	6.35	5.04	0.46	0.56	0.21	0.42	3.50
		<i>4</i>	83	4.26	5.04	0.40	0.49	0.27	0.55	0.76
		<i>5</i>	84	4.30	5.04	0.34	0.45	0.27	0.57	0.45
	Median									
		<i>1</i>	86	5.21	5.04	0.39	0.48	0.25	0.59	1.85
		<i>2</i>	86	4.32	5.04	0.34	0.43	0.28	0.62	1.54
		<i>3</i>	83	5.17	5.04	0.44	0.52	0.24	0.46	1.81
		<i>4</i>	84	4.16	5.04	0.37	0.47	0.28	0.49	0.54
		<i>5</i>	83	4.63	5.04	0.40	0.51	0.26	0.47	1.57

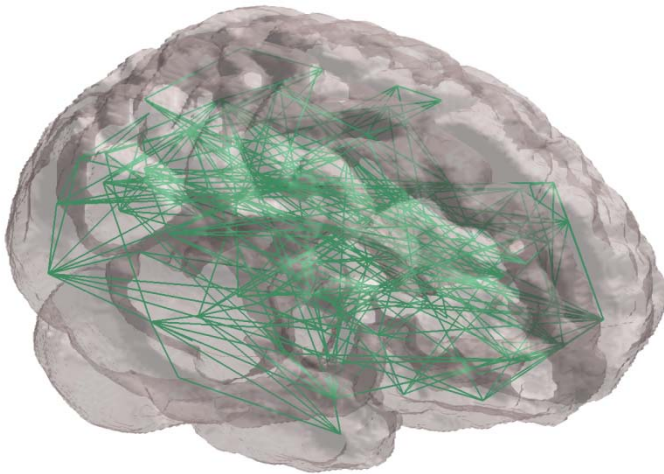


Fig. 1. Network of subject 10 in brain space.

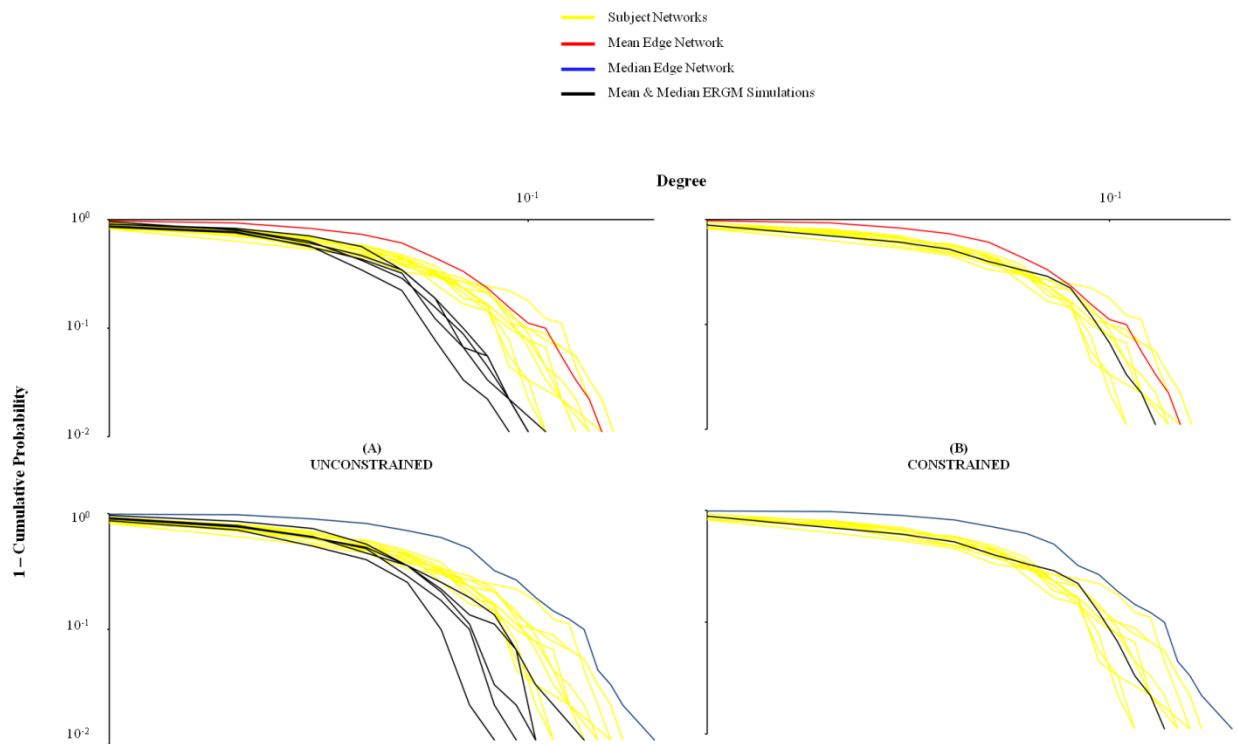


Fig. 2. Degree distribution plots for the 10 subjects' networks, the edge-based *mean* and *median* correlation networks, and **a)** the unconstrained *mean ERGM* and *median ERGM* simulation-based networks and **b)** the degree-constrained *mean ERGM* and *median ERGM* simulation-based networks.

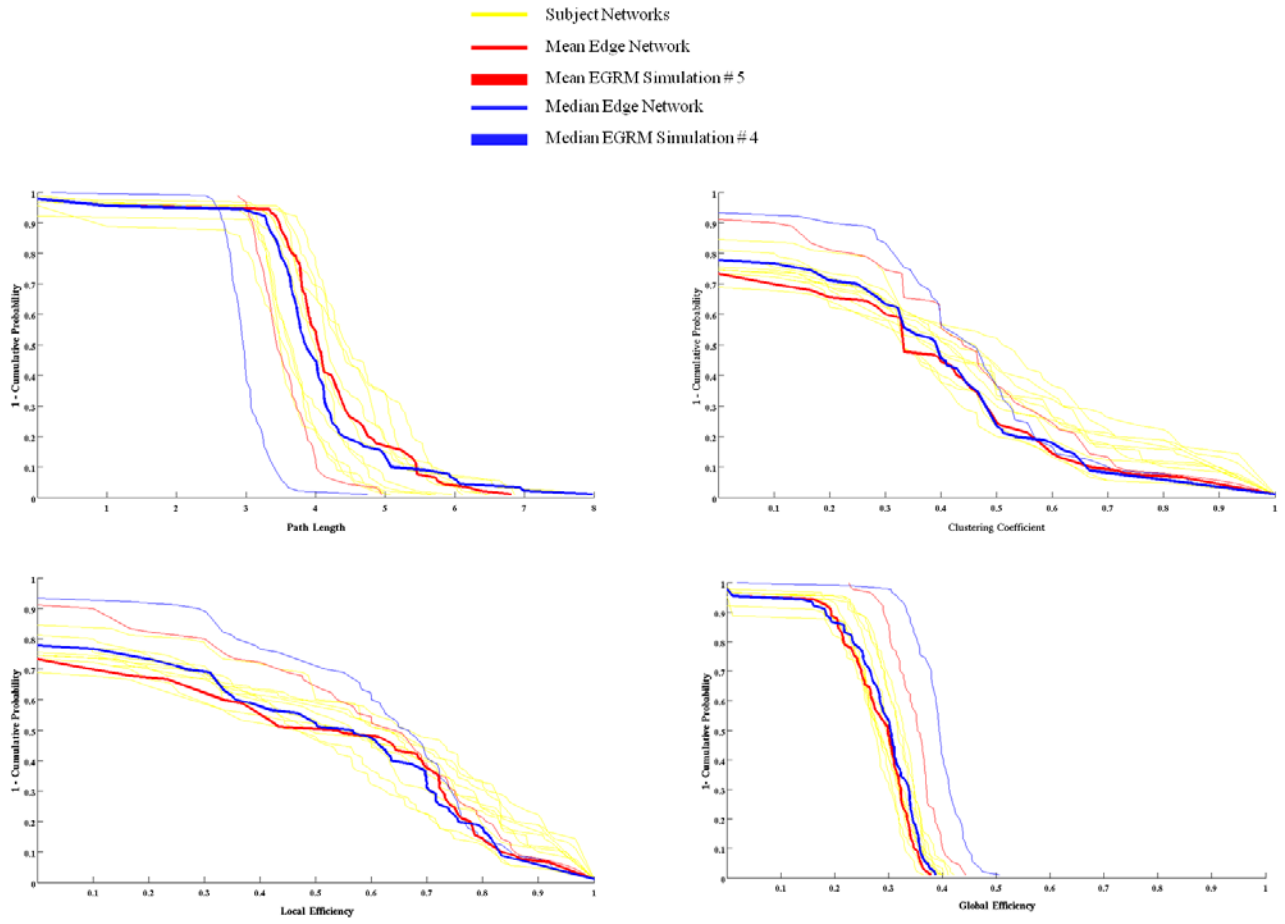


Fig. 3. Nodal distributions of path length (L), clustering coefficient (C), global efficiency (E_{glob}), and local efficiency (E_{loc}) for the 10 subjects' networks, *mean* and *median* correlation networks, and *mean ERGM* network #5 and *median ERGM* network #4.

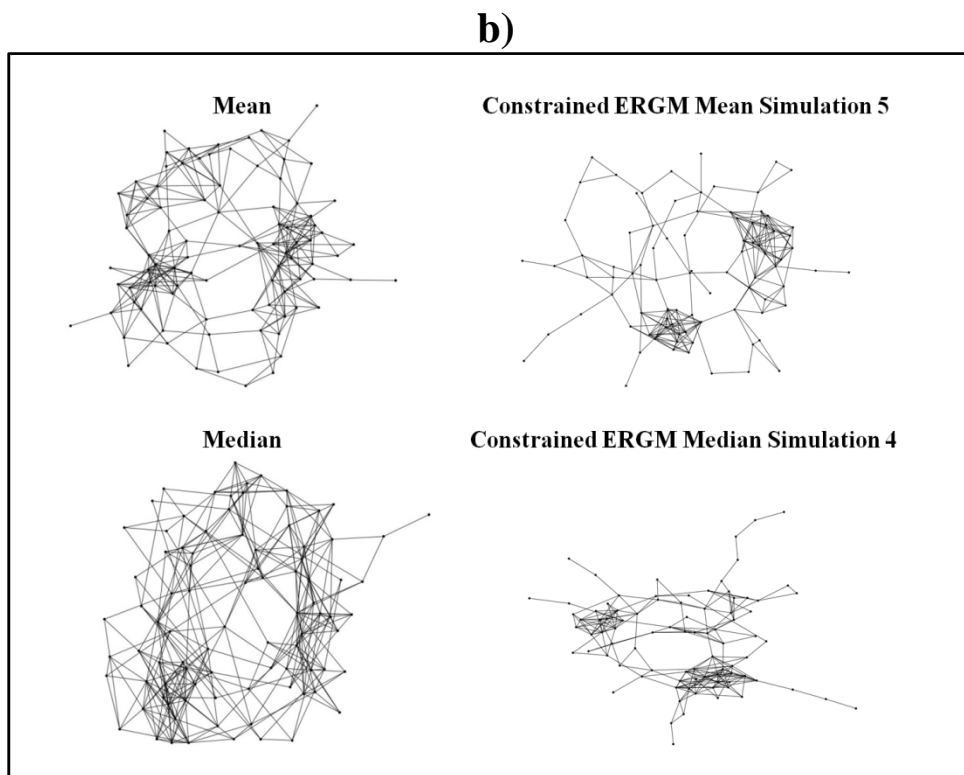
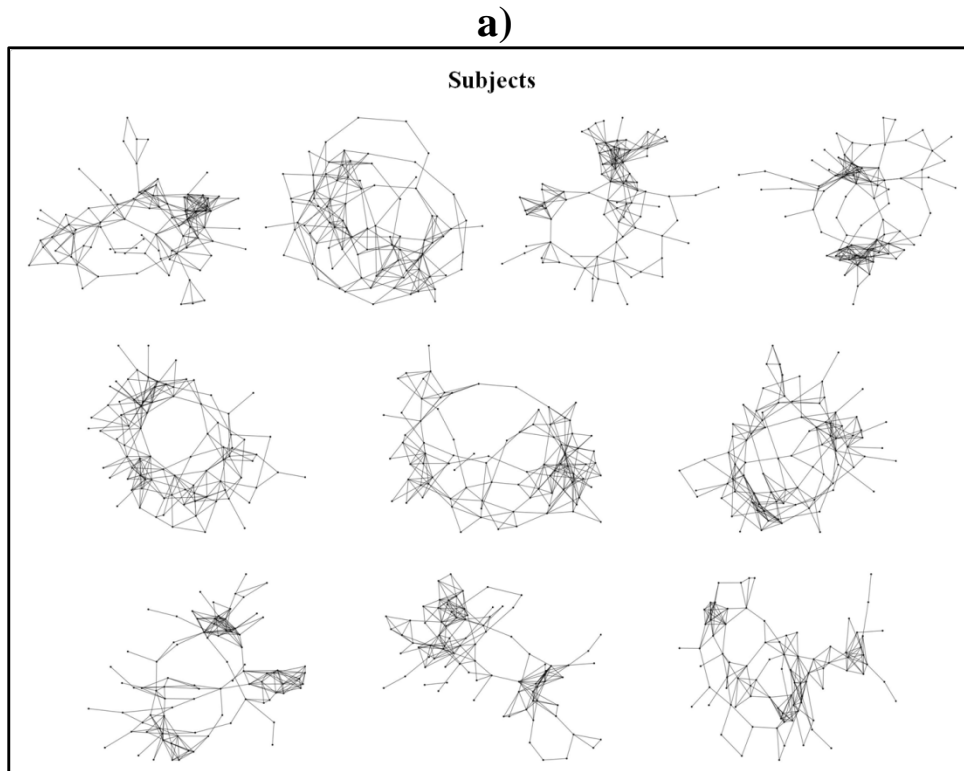


Fig. 4. Harel-Koren Fast Multiscale graphs for **a)** the 10 subjects' networks and **b)** the *mean* and *median* correlation networks, constrained *mean ERGM* network #5, and constrained *median ERGM* network #4.